ChemComm

This article is part of the

Microfluidics

web themed issue

Guest editors: Andrew deMello, Florian Hollfelder and Klavs Jensen

All articles in this issue will be gathered together online at
www.rsc.org/microfluidics

ChemComm

Dynamic Article Links

Cite this: *Chem. Commun.*, 2012, **48**, 9144–9146

www.rsc.org/chemcomm

COMMUNICATION

Lab-chip HPLC with integrated droplet-based microfluidics for separation and high frequency compartmentalisation†‡

Jin-Young Kim,[a] Soong-Won Cho,[b] Dong-Ku Kang,[c] Joshua B. Edel,[b] Soo-Ik Chang,[d] Andrew J. deMello[e] and Danny O'Hare*[a]

Received 25th May 2012, Accepted 23rd July 2012
DOI: 10.1039/c2cc33774f

We demonstrate the integration of a droplet-based microfluidic device with high performance liquid chromatography (HPLC) in a monolithic format. Sequential operations of separation, compartmentalisation and concentration counter were conducted on a monolithic chip. This describes the use of droplet-based microfluidics for the preservation of chromatographic separations, and its potential application as a high frequency fraction collector.

Recent years have seen considerable interest in microfabricated systems and their applications in chemical and biological analysis.[1–8] Inevitably this has led to a growing interest in translating established chromatographic methods to planar chip formats since these techniques play such a prominent role in modern bioanalysis.[9–11] However, the operation of chromatography on the microscale has its own problems. Dispersion of separated bands results from molecular diffusion as well as the dead volume of the channel, detector and collector after separation and can degrade the analytical quality.[12,13]

Recently, the manipulation of multiphase (or segmented) flows within microfluidic channels has been a focus of intense interest.[14–16] Flow segmentation allows compartmentalisation of reagent volumes from fL to μL within a continuous and immiscible fluid, the production of monodisperse droplets at high frequencies, and the accurate control of droplet contents.[2,16]

Integration of droplet-based microfluidics with HPLC has the potential to dramatically reduce dispersion and minimise dead volume effects by using droplets to collect fractions of the column effluent. This preserves the chemical identity of each fraction allowing further analysis downstream or offline. Niu *et al*. have previously described the compartmentalisation of the separated analytes in two-dimensional separations using discrete components.[17] Edgar *et al*. have compartmentalised CE separated analytes using droplets.[13] Whilst there have been reports of droplet-based fraction collectors for HPLC,[18,19] these investigators used commercially available HPLC columns and discrete segmented flow modules. Integration of both functions on a single planar device has not been reported and represents a significant challenge due to the high pressures used in chip-based HPLC.

Most microfluidic devices are made from polydimethylsiloxane (PDMS) because of its compatibility with simple lab-scale fabrication procedures. Unfortunately, PDMS is not suitable for HPLC due to the high operating pressure, typically up to 15 MPa during routine separation,[20] and this has hindered hybrid device development.

As an alternative, we propose the use of thermoset polyester (TPE) which overcomes such limitations whilst retaining the advantages associated with rapid prototyping.[21–23] This communication describes the development of a multilayer TPE microfluidic device which combines HPLC with downstream droplet generation. Proof-of-principle separations of fluorescent dyes were used to characterise the effects of the interfacing on dispersion.

Our device consists of two layers: an HPLC channel for separation and a flow-focusing channel for droplet generation (Fig. 1). Inset (b) shows an image of the 1 mm wide separation channel packed with 5 μm C18 particles for HPLC in the first layer, and the 250 μm wide droplet channel in the second layer on top of the separation channel. The mobile phase and solutions for analysis are introduced through the mobile phase inlet into the separation channel. Following separation by reverse phase HPLC, the analytes flow to the upper layer through the inlet of the droplet channel where compartmentalisation occurs.

We have previously shown that, in comparison to PDMS, TPE has excellent mechanical properties as a substrate material, withstanding pressures up to 18 MPa.[23]

Burst pressure test demonstrated that the completed device can withstand approximately 8 MPa (ESI‡, Fig. S3). Although lower than 15 MPa, it is sufficient for compartmentalisation

[a] *Department of Bioengineering, Imperial College London, London SW7 2AZ, UK. E-mail: d.ohare@imperial.ac.uk*
[b] *Department of Chemistry, Imperial College London, London SW7 2AZ, UK*
[c] *Department of Pharmaceutical Sciences, University of California, Irvine, CA 92697, USA*
[d] *Department of Biochemistry, Chungbuk National University, Cheongju, Chungbuk 361-763, Korea*
[e] *Institute for Chemical and Bioengineering Department of Chemistry and Applied Biosciences, ETH Zurich, CH-8093, Zurich, Switzerland*
† This article is part of the ChemComm 'Microfluidics' web themed issue.
‡ Electronic supplementary information (ESI) available: Experimental details and additional results. See DOI: 10.1039/c2cc33774f

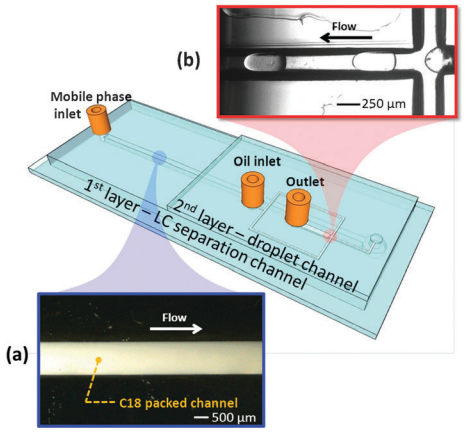

Fig. 1 Schematic of the fabricated hybrid device, (a) an image of the C18 packed 1 mm wide separation channel and (b) the 250 µm wide droplet channel. Arrows show the direction of fluid flow.

after HPLC because the pressure at the HPLC outlet is lower than 1 MPa. Moreover it is sufficient to generate droplets at high frequency (over 1 kHz) which typically requires total pressure in excess of 1 MPa.[23]

Fig. 2(a) shows the laser-induced fluorescence (LIF) detection locations before and after compartmentalisation into droplets. When separated using the on-chip HPLC, AF 488 and FITC were eluted with retention times of 50 s and 335 s, respectively, as shown in Fig. 2(b) with a resolution of 2.58. Fig. 2(b) and (c) show the segmented analytes observed at point (ii) and the continuous signal associated with the analytes moving through the separation column at point (i). To investigate diffusional band broadening, the chromatograms in (b) and (c) were quantitatively compared using the maximum values of each droplet signature.

A digital maximum filter with a 40 point window size (Igor Pro 6), slightly longer than the maximum interval between the droplets, was applied. As shown in Fig. 2(d), the two chromatograms were strongly correlated, with a slope of 1.0025 ± 0.000185 and a correlation coefficient of 0.98. Furthermore the number of theoretical plates (N) for each peak in both the chromatograms was compared using eqn (1),[12,24]

$$N = 5.54\left(\frac{t_r}{w_{0.5}}\right)^2 \qquad (1)$$

where t_r is the retention time and $w_{0.5}$ is the peak width at half height. The AF 488 and FITC peaks yield plate numbers of 19 and 63, respectively, for both the continuous and droplet flows indicating that no significant dispersion occurs after separation and during compartmentalisation. Doubtless the separation could be further improved by changing the packing method or reducing the particle size and size distribution of the beads. Nonetheless the observed separations show similar figures of merit to those observed for droplet flow fractionation from conventional columns.[18,19]

The slope of the correlation plot (Fig. 2) is close to 1 showing that the sensitivity of the LIF detection was similar for the maximum intensity of the droplets and continuous flow. The path length for both absorption and re-emission at the maximum would be similar for both situations. Fluorescence emission is isotropic with the photon flux scaling

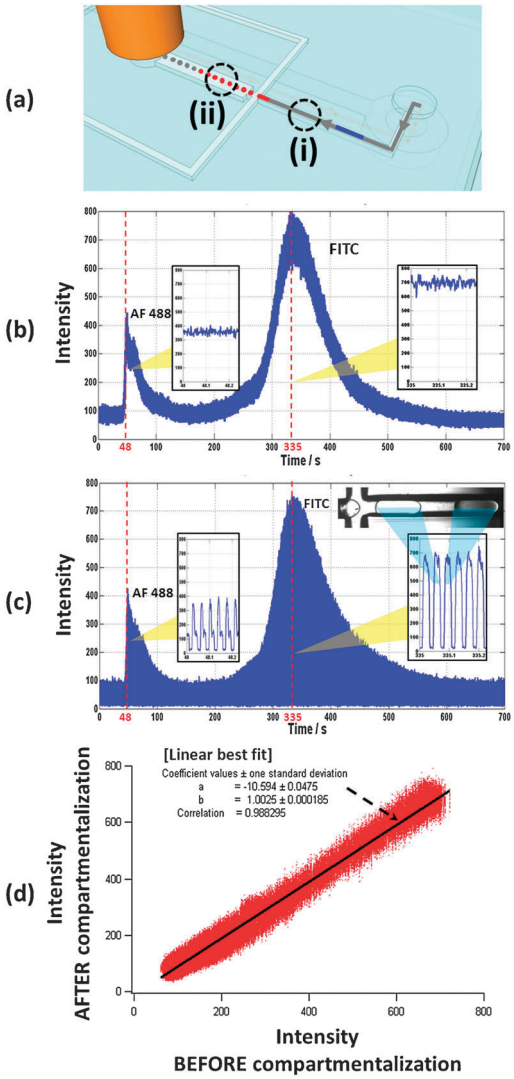

Fig. 2 LIF detection of AF 488 and FITC, (a) schematic of the movement of fluids in the channels and the two laser detection points, (b) the chromatograms of the separated dyes from point (i), (c) compartmentalised dyes from point (ii) and (d) linear best fit between both chromatograms.

with the mean chord length, $4V/S$ where V is the volume and S is the surface area, provided the concentration is low.[25] For a droplet of radius r, compared with a cube of side $2r$ the mean chord length is essentially the same. The slope of the correlation plot shows that there are no significant lensing effects, at least for the solvents and oils used in these experiments.

Fraction composition can be controlled straightforwardly and easily by adjusting the oil flow rate. To demonstrate this, three different oil flow rates (50, 75 and 100 µl min^{-1}) were used with a running buffer flow rate of 50 µl min^{-1} (approximately 1.6 MPa back pressure) (Fig. 3). Fig. 3 shows optical images and fluorescent signals of the FITC containing droplets generated by each oil flow rate. Fraction composition can be controlled straightforwardly and easily by adjusting the oil flow rate. To demonstrate this, three different oil flow rates (50, 75 and 100 µl min^{-1}) were used with a running buffer flow rate of 50 µl min^{-1} (approximately 1.6 MPa back pressure) (Fig. 3).

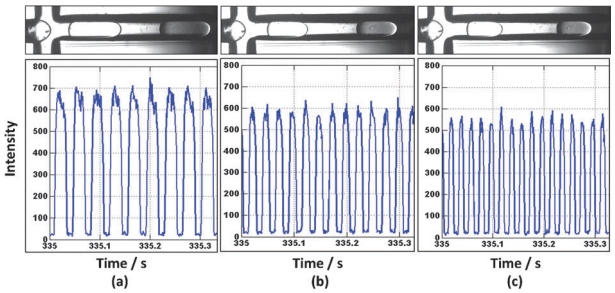

Fig. 3 Optical images and fluorescence signals of the FITC droplets as a function of oil flow rates, (a) 27 Hz by 50 μl min^{-1}, (b) 39 Hz by 75 μl min^{-1}, (c) 50 Hz by 100 μl min^{-1}.

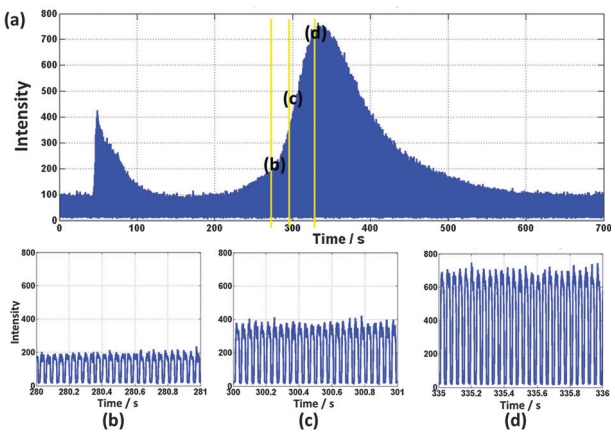

Fig. 4 Concentration gradient of FITC droplets, (a) selected times on the FITC peak and fluorescence signals of the FITC droplets at (b) 280 s, (c) 330 s and (d) 335 s.

Fig. 3 shows optical images and fluorescent signals of the FITC containing droplets generated by each oil flow rate.

It can be seen that the droplet size decreases as the generation frequency increases with increasing oil flow rate. As a result, the AF 488 peak could be segmented and stored within 1000–2000 droplets at rates up to 50 Hz. In the case of FITC, approximately 10 000 to 20 000 microdroplets were generated by the wider peak for about 370 s in this frequency range. Furthermore as shown by the plate number N and the linear fitting for the three different chromatograms, compartmentalisation led to droplet compositions faithful to the continuous flow chromatogram without additional band-broadening (ESI‡, Fig. S4, S5 and S6). In this way, separated analytes can be successfully compartmentalised into droplets of a defined volume. Moreover since concentrations in the separated bands are Gaussian at the column outflow, variation in concentration between droplets can be controlled at high speed.[26] This process can be observed in Fig. 4 which shows segmented peaks taken at three different times (200 s, 300 s and 335 s) for the separated FITC peak. The data show precise and accurate droplet generation comprising different concentrations of FITC on each occasion.

Sequential operations of separation, compartmentalisation and concentration counter have successfully been integrated on a monolithic chip. This confirms the potential of droplet-based microfluidics for preservation of chromatographic separations and its ability to act as a high frequency fraction collector in a single hybrid device.

This work was supported by the Global Research Laboratory Program of the National Research Foundation of Korea (NRF) funded by the Ministry of Education, Science, and Technology (MEST) of Korea (Grant Number K20904000004-11A0500-00410).

Notes and references

1 G. M. Whitesides, *Nature*, 2006, **442**, 368–373.
2 A. J. deMello, *Nature*, 2006, **442**, 394–402.
3 J. Hong, M. Choi, A. J. deMello and J. B. Edel, *BioChip J.*, 2009, **3**, 203–207.
4 A. Arora, G. Simone, G. B. Salieb-Beugelaar, J. T. Kim and A. Manz, *Anal. Chem.*, 2010, **82**, 4830–4847.
5 G. B. Salieb-Beugelaar, G. Simone, A. Arora, A. Philippi and A. Manz, *Anal. Chem.*, 2010, **82**, 4848–4864.
6 C. Lim, J. Hong, B. G. Chung, A. J. deMello and J. Choo, *Analyst*, 2010, **135**, 837–844.
7 X. C. I. Solvas and A. deMello, *Chem. Commun.*, 2011, **47**, 1936–1942.
8 S. W. Cho, D. K. Kang, J. Choo, A. J. deMello and S. I. Chang, *BMB reports*, 2011, **44**, 705–712.
9 J. K. Liu, C. F. Chen, C. W. Tsao, C. C. Chang, C. C. Chu and D. L. Devoe, *Anal. Chem.*, 2009, **81**, 2545–2554.
10 A. Manz, Y. Miyahara, J. Miura, Y. Watanabe, H. Miyagi and K. Sato, *Sens. Actuators, B*, 1990, **1**, 249–255.
11 G. Ocvirk, E. Verpoorte, A. Manz, M. Grasserbauer and H. M. Widmer, *Anal. Methods Instrum.*, 1995, **2**, 74–82.
12 S. Lindsay and ACOL (Project), *High performance liquid chromatography*, Published on behalf of Thames Polytechnic, London, by Wiley, Chichester, England, New York, 2nd edn, 1992.
13 J. S. Edgar, G. Milne, Y. Q. Zhao, C. P. Pabbati, D. S. W. Lim and D. T. Chiu, *Angew. Chem., Int. Ed.*, 2009, **48**, 2719–2722.
14 H. Song, D. L. Chen and R. F. Ismagilov, *Angew. Chem., Int. Ed.*, 2006, **45**, 7336–7356.
15 Y. Schaerli and F. Hollfelder, *Mol. BioSyst.*, 2009, **5**, 1392–1404.
16 J. Hong, M. Choi, J. B. Edel and A. J. deMello, *Lab Chip*, 2010, **10**, 2702–2709.
17 X. Z. Niu, B. Zhang, R. T. Marszalek, O. Ces, J. B. Edel, D. R. Klug and A. J. Demello, *Chem. Commun.*, 2009, 6159–6161.
18 A. B. Theberge, G. Whyte and W. T. S. Huck, *Anal. Chem.*, 2010, **82**, 3449–3453.
19 S. Hamed, B. Shay and A. S. Basu, *2011 Annual International Conference of the IEEE Engineering in Medicine and Biology Society (Embc)*, 2011, pp. 8396–8399.
20 S. Ehlert and U. Tallarek, *Anal. Bioanal. Chem.*, 2007, **388**, 517–520.
21 G. S. Fiorini, R. M. Lorenz, J. S. Kuo and D. T. Chiu, *Anal. Chem.*, 2004, **76**, 4697–4704.
22 J. H. Seo, P. L. Leow, S. H. Cho, H. W. Lim, J. Y. Kim, B. A. Patel, J. G. Park and D. O'Hare, *Lab Chip*, 2009, **9**, 2238–2244.
23 J. Y. Kim, A. J. deMello, S. I. Chang, J. Hong and D. O'Hare, *Lab Chip*, 2011, **11**, 4108–4112.
24 R. F. Venn, *Principles and practice of bioanalysis*, Taylor & Francis, 2000.
25 A. Mazzolo, *Ann. Nucl. Energy*, 2008, **35**, 503–506.
26 O. J. Miller, A. El Harrak, T. Mangeat, J. C. Baret, L. Frenz, B. El Debs, E. Mayot, M. L. Samuels, E. K. Rooney, P. Dieu, M. Galvan, D. R. Link and A. D. Griffiths, *Proc. Natl. Acad. Sci. U. S. A.*, 2012, **109**, 378–383.

